Journal of Alloys and Compounds 505 (2010) 692–697

Contents lists available at ScienceDirect

Journal of Alloys and Compounds

journal homepage: www.elsevier.com/locate/jallcom

Effect of APC addition on stability of nanosize precursors in sol–gel processing of SiC nanopowder

A. Najafi[a,*], F. Golestani-Fard[a,b], H.R. Rezaie[a,b], N. Ehsani[a]

[a] School of Metallurgy and Materials Engineering, Iran University of Science and Technology, Daneshgah St., 16844, Narmak, Tehran, Iran
[b] Center of Excellence for Advanced Materials, Iran University of Science and Technology, 16845-195, Narmak, Tehran, Iran

ARTICLE INFO

Article history:
Received 24 March 2010
Received in revised form 13 June 2010
Accepted 19 June 2010
Available online 1 July 2010

Keywords:
Nanostructured materials
Sol–gel processes
Chemical synthesis
Scanning electron microscopy (SEM)
Transmission electron microscopy (TEM)
X-ray diffraction

ABSTRACT

Dispersion characteristics of a sol were assessed in terms of surface charge, particles size and rheological measurements. TEOS and phenolic resin were used as silicon and carbon sources, respectively, for preparing SiC nanopowder. APC was used as a dispersant agent. APC significantly increased the surface charges of the particles in intermediate pH and moreover as an acidic agent shifted pH to lower values. DLS measurements indicated more stability and controllable size of particles in the presence of APC. At pH < 4, size of particles was measured to be less than 10 nm. Rheometry measurements for sol showed that the viscosity increased and stability of particles decreased in intermediate pH. Electrokinetic measurements were used to determine adsorption specific free energy (ΔG°_{sp}) between surface sites and adsorbing dispersant. Results showed a negative amount (−1.57 RT) that indicates a favorable interaction between particle surface and dispersant. FTIR of the dried gel powder indicated that (Si–O–C) bonds were formed due to hydrolysis and condensation reactions. XRD studies showed that the synthesized powder which was heat treated in 1500 °C for 1 h consists of β-SiC phase. SEM observations showed that the β-SiC particles agglomerated with a particle size less than 100 nm.TEM analysis indicated a semi-spherical morphology and mean size of 30–50 nm for β-SiC particles.

1. Introduction

Recently, carbide materials have been used for many applications in advanced ceramics industry due to their attractive characteristics. Silicon carbide is one of the most important carbide materials because of its unique properties and is known as an important non-oxide ceramic with high melting point (2827 °C), high hardness, high wear resistance, low thermal expansion coefficient, good chemical resistance and good thermal conduction in ceramic industry [1–3].

This ceramic material is used in electrical industries, high temperature engineering ceramic devices and as reinforcement for ceramic composites [4–7]. Different methods which were used for SiC particles synthesis include Si metal direct carbonization, chemical vapor deposition (CVD), carbothermal reduction of silicon dioxide and sol gel technique. Some of these methods are accompanied with shortcomings, these include high cost, low efficiency and high impurity.

The sol–gel process, however, has proved a unique method for synthesis of nanopowder, this method has several outstanding features such as high purity [8], high chemical activity, improvement of powder sinterability, possibility for particles mixing at molecular scale. A sol gel process using metal alkoxides has been widely applied for the synthesis of ideal powders; homogeneous, size and shape controlled, and high purity [9]. The flexibility of sol–gel chemistry, involving silicon alkoxides as precursors and the ability to prepare stable inorganic matrices close to room temperature are compatible with a wide variety of dyes [10].

Aelion et al. were among the first to investigate the kinetics of hydrolysis and condensation of TEOS. The rate and extent of the hydrolysis reaction were found to be influenced by the strength and concentration of the acid or base catalyst while temperature and solvent were of secondary importance [11]. Dispersion of nano/colloidal size particle suspensions in aqueous and non-aqueous systems is crucial for the success of many advance and modern manufacturing processes in a variety of applications. With a rapid trend towards miniaturization and the utilization of nanopowders, understanding of their suspension behavior and role of cohesion are of paramount importance. It is very difficult to keep nanoparticulate system, as discrete primary particles in the dispersion, as it tends to form lose agglomerates. In general, colloidal and nanosuspensions are thermodynamically unstable due to large surface energy associated with finely dispersed systems. However, these dispersions can show kinetic stability if required energy barrier against agglomeration/aggregation can be provided through

---

* Corresponding author. Tel.: +98 2173912834/9121032632; fax: +98 2177240291.
E-mail address: ab_najafi@iust.ac.ir (A. Najafi).

0925-8388/$ – see front matter © 2010 Elsevier B.V. All rights reserved.
doi:10.1016/j.jallcom.2010.06.116

forces such as electrical double layer, electrostatic forces. This area is attracting increasing attention from a variety of interdisciplinary fields of research [12].

A sol, which forms a gel, is a colloidal suspension of solid particles in a liquid. According to the classical concepts of colloid chemistry, a colloid is a suspension in which the dispersed phase is so small (1–1000 nm) that the gravitational forces are negligible and interactions are dominated by short-range forces, such as van der Waals attraction and surface charges [13]. The use of an aqueous polymeric surfactant allows the achievement of highly stable suspensions for all nanoparticle SiC samples in the considered range of concentration [14].

Ponton et al. reported on the study of gelation of silica-based materials by small amplitude oscillatory shear measurements. The gelation time has been determined from the variation of the elastic loss moduli with time at different frequencies. Investigations are made for different water amounts, monomer concentrations, and different temperatures [15]. To increase the precision of viscosity measurements Adamczyk et al. chose the capillary measurement technique using a new homemade apparatus, largely eliminating suspension sedimentation effects. This is vital in view of further studies on rheological properties of mineral suspensions in colloid silica [16]. Arriagada et al. developed a novel synthesis route for silica nanoparticles with a wide range of water/surfactant ratio. They showed that particle size and size distribution are complex functions of the initial micro emulsion formulation [17].

Zackrisson et al. studied effects of particle concentration on the irreversible aggregation of colloidal silica using in situ destabilization via the ionic strength increase derived from the enzymatic hydrolysis of urea by urease. Comparisons are made with dispersions destabilized by direct addition of salt solutions, which gel under very different condition [18]. Martin et al. investigated the effect of pressure and temperature on SiC nanopowders obtained from silica sol and sugar [19]. Tamon et al. synthesized silica alcogels by the sol–gel polymerization of TEOS using HCl and NH_3 as catalysts and elucidated the influence of the hydrolysis time on the gelation time and the visible light transmission of alcogels [20].

In this study, the dispersion behavior of nanosize particles in the presence of ammonium poly-carboxylate (APC) as dispersant agent is explained. Understanding the importance of the colloid science and technology for obtaining suspensions without particle agglomerates is the main aim of this study since it could result in products with appropriate nanostructure in colloidal processes.

2. Materials and methods

2.1. Materials

Tetraethyl orthosilicate (TEOS, Merck Ag Germany), choloridric acid and NaOH (HCl, NaOH, Merck Ag Germany) as catalysts solutions, Phenolic resin (Resol, RIL 800 Resitan Co., Iran), ethanol (Merck Ag Germany), acetone (Merck Ag Germany) as resol solvent and distilled water were used in this study, and ammonium poly-carboxylate (APC, D-305) with molecular weight of about 8000–10,000 g/mol was used as dispersant agent. According to reaction (1), the structure of ammonium poly-carboxylate and decomposition reactions demonstrate that carboxylic groups are functional ones which can be decomposed as $RCOO^-$ [12].

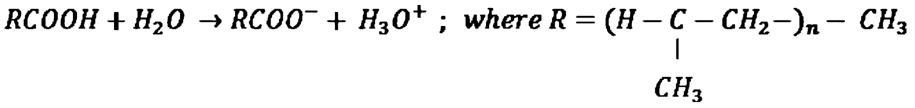

$$RCOOH + H_2O \rightarrow RCOO^- + H_3O^+ \ ; \ \text{where } R = (H - \underset{\displaystyle CH_3}{\overset{}{C}} - CH_2-)_n - CH_3$$

2.2. Methods

At first, 60 ml TEOS, 40 ml water and 30 ml ethanol were mixed and then a solution containing 50 g phenolic resin in 100 ml acetone was added to it. This solution under a reflux condition was homogenized by a magnetic stirrer and its pH was controlled by introducing the sufficient amounts of catalyst (HCl and NaOH). Also for sol stabilization the dispersant agent (0.05 mol/l) was added to it. Subsequently, during hydrolysis reactions and $Si(OH)_4$ particles formation, the solution was dealcoholized at 40 °C. Then, it was diluted by water to prevent faster gelation resulted from diminishing alcohol. Final solution was included of very small and homogenous $Si(OH)_4$ particles and phenolic resin which resolved completely.

The temperature elevation resulted in particles connection and polymers formation with siloxan bonds (Si–O–Si). These polymers joint together and made a chained structure in which water was trapped. The carbon phase was merged inside the polymer structure. Then the gel was dried and xerogel was produced.

In order to remove the structural water and organic matters, resulted powder was pyrolyzed at 700 °C for 1 h under Ar atmosphere. The obtained powder had black color. Then the pyrolyzed powder was heat treated at 1500 °C for 1 h with a heating rate of 10 °C/min in an electrical furnace (carbolite 1600) in alumina crucible at Ar flow of 100 ml/min.

The resulted powder was greenish. Various characterization methods including particle charge detector (Zeta Sizer, Malvern DTS) were used to perform surface charge measurements. This detector acts on basis of current potential measurement which is created when polar ions are separated in double electric layers from charged particles in liquid. Rheometry analysis was performed (Phisica, MCR300) under thermally controlled conditions from ambient temperature to 120 °C. The viscosity was measured with constant shear rate of $2600\,s^{-1}$ at 25 °C. The rheology behavior of suspensions contained nanosize particles was studied by measuring viscosity and shear tension as a function of shear and pH amounts. Sol stabilization was investigated by zeta potentiometry using Zeta sizer Malvern DTS. Dynamic light scattering analysis (DLS, Malvern DTS) was performed for measuring the particles size and stability in colloidal system. In this method, the solubility rate is measured on the basis of the illumination of laser beam with less than 100 nm wavelength in the sol containing nanosize particles. The suspended particles in the sol are constantly moving due to Brownian motions, and they experience contacts with other particles. The relationship between particles size and their Brownian motion speed is calculated from the Stokes–Einstein (Eqs. (1) and (2)) [21].

$$D = \frac{k_B T}{6\pi\eta r} \tag{1}$$

$$\mu_p = \frac{1}{6\pi\eta r} \tag{2}$$

where D is the diffusion coefficient, μ_p is particle mobility, T is the solution temperature, η is the solution viscosity and r is the particle radius. FTIR analysis (FTIR, Shimadzu, 8400S) for bonds specifications, X-ray diffractions analysis (XRD, Philips Xpert) for phase studies of synthesized powder, scanning electron microscopy (FE-SEM, S4160-Hitachi) and transmission electron microscopy (TEM, Philips) for structural investigations were performed.

3. Results and discussion

3.1. Nanosize particles surface chemical properties

The stability of suspensions containing nanosize particles depends on the amounts of surface charge. Silica alkoxides in the presence of water molecules are hydrolyzed according to reaction (3) and OR groups are replaced by OH ions. This reaction results in silanol groups (Si-OH) which are naturally amorphous. In pH range less than that of point zero charge (PZC), silanol groups react with H^+ ions and form ($Si\text{-}OH_2{}^+$) groups [12] and in pH amounts more than PZC they react with OH^- ions and results in ($Si\text{-}O^-$) groups formation (reactions (4) and (5)).

$$Si\text{-}OR + H_2O \rightarrow Si\text{-}OH + ROH \tag{3}$$

$$Si\text{-}OH + H^+ \rightarrow Si\text{-}OH_2{}^+ \quad pH < PZC \tag{4}$$

$$Si\text{-}OH + OH^- \rightarrow Si\text{-}O^- + H_2O \quad pH > PZC \tag{5}$$

The charge amounts in different pHs corresponding to reactions (4) and (5) are shown in Table 1. Silanols are relatively acidic and easily react with OH^-. As it can be seen, the PZC can be found in the pH range of 2–2.5. By increasing the pH, higher negative surface charges are obtained. The results show that the nanosize particles exhibit a floculant effect in solution at pHs of 4–7. This effect leads to strong attraction between particles and alleviates the sol stability.

Table 1
Experimental data of nanosize particles surface charge density.

pH	Surface charge observation density (*C*/g)	
1.50	0.3142	
1.75	0.2412	
2.00	0.0012	
2.50	−0.0107	
3.20	−0.0120	$pH_{PZC} = 2–2.5$
4.00	−0.0340	
5.40	−0.0980	
6.90	−0.1960	

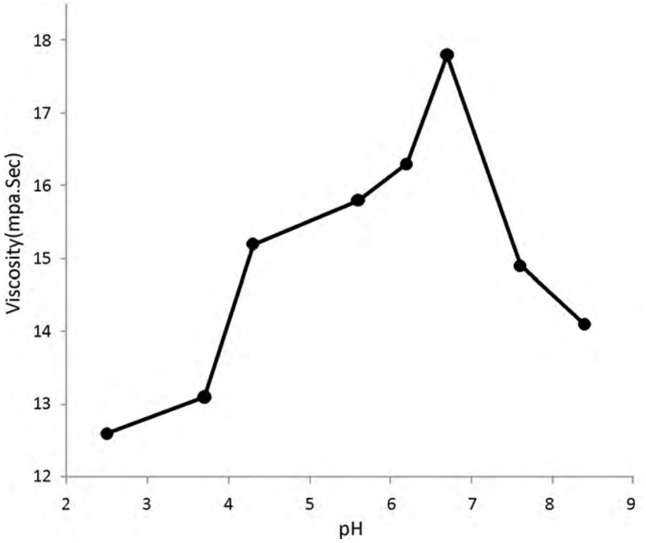

Fig. 2. Effect of pH on suspension viscosity.

The surface charge variations (*C*/g) as a function of pH amounts with and without dispersant are plotted in Fig. 1. The amount of pH_{PZC} in the absence of dispersant agent is in the range of 2–2.5. The surface charge is positive at pH amounts lower than PZC and is negative at higher ones. Addition of dispersant APC yields changes in surface charge, and the amount of negative surface charge will be increased because of dispersant adsorption on nanosize particles' surfaces. APC dispersant changes pH in the sol and it becomes more acidic with lower pH amounts. It is clear that the surface charge on nanosize particles is negative for a wide pH range (>2.5). More changes in pH amounts demonstrate that interaction between particles and dispersant APC probably has chemical nature. The chemical adsorption process which was involved in formation of chemical bonds is known as an irreversible surface adsorption process. Since, unfortunately, there is not any report on surface charge density for nanosize precursors particles during SiC synthesis, we cannot compare the present data and give in depth comments.

3.2. Rheological behavior

The viscosity variations of sol containing nanosize particles as a function of pH are shown in Fig. 2 at constant shear rate of 2600 s^{-1}. As it is seen, the highest viscosity belongs to the pH in range of 4–7. In other words, particles attraction inside the sol is increased in this range, and mobility is decreased. According to Eqs. (1) and (2), as sol viscosity increases at constant temperature, particles mobility and stability decrease. Therefore, sol stability is lower for this pH range. Also, the suspension is well dispersed in extremely high and extremely low pH amounts and sol viscosity is low and its stability increases.

Fig. 2 could be confirmed by Fig. 3 which shows zeta potential variation vs. pH. This figure shows that at pH lower than 4 the ideal zeta potential was achieved for a stable colloidal system. At pH values of 4–7, the zeta potential tends to zero and minimum stability was achieved. In this condition the particles agglomeration occurred. At pH values more than 7, the absolute value of zeta potential increased and formed stable colloidal system.

3.3. Adsorption free energy calculations using electrokinetic results

It is well established that the interaction between double electric layers plays an important role on dispersants adsorption. Electrokinetic measurements are one of the most important methods for studying dispersants interaction which is performed on the solution containing dispersants. Electrokinetic data show that the surface charge on particle surface changes by addition of dispersant for systems with chemical adsorption. This effect can be shown by Eqs. (6) and (7) based on special interactions between surface sites and dispersant based on electric double layer theory [12]:

$$\Delta \mathrm{pH} = 1.0396 C_o \exp\left(-\frac{\Delta G^\circ{}_{sp}}{RT}\right) \qquad (6)$$

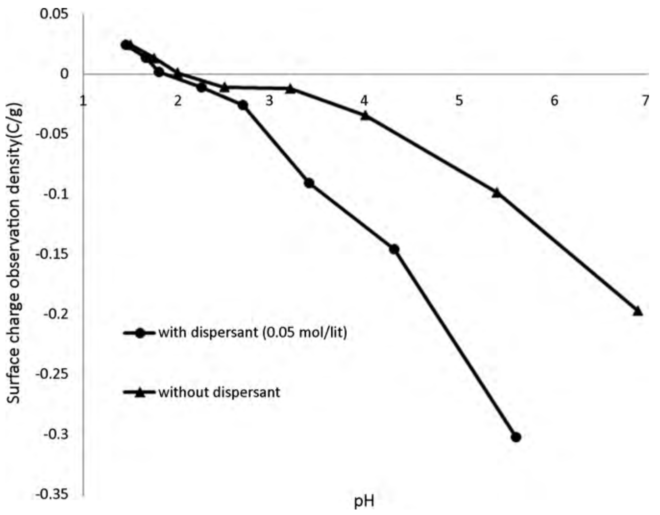

Fig. 1. Effect of pH on surface charge density with and without dispersant.

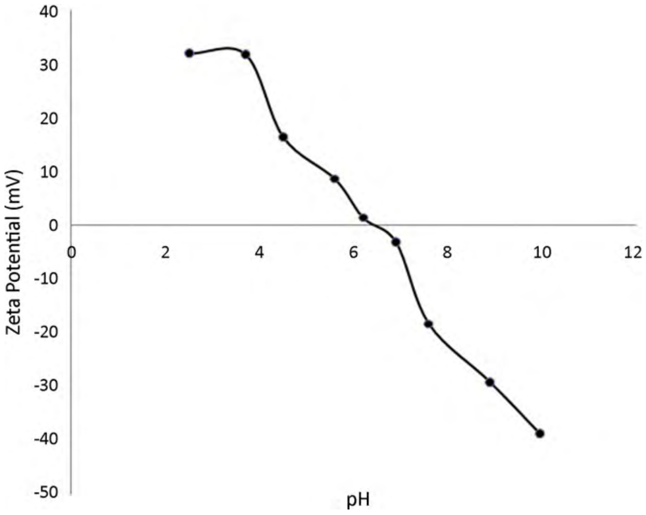

Fig. 3. Zeta potential variation vs. pH.

Table 2
Specific free energy of interaction between particles and APC.

ΔG°_{sp} (unit RT)	ΔpH	pH	
		No dispersant	Sol/APC
−1.570	0.250	2.500	2.250
−2.264	0.500	3.200	2.700
−2.440	0.600	4.000	3.400
−3.050	1.100	5.400	4.300
−3.210	1.300	6.900	5.600

or

$$\Delta G^\circ_{sp} = -RT(\ln \Delta\text{pH} - \ln C_o - \ln 1.0396) \quad (7)$$

where ΔG°_{sp} is the free energy of interaction between particles surface and dispersant, ΔpH is sol pH changes due to dispersant addition, C_o is the dispersant concentration (0.05 mol/l), and R and T are standard coefficient of gas and temperature (K), respectively. Interaction happens with changing in surface charge amounts. This change is related to ΔG°_{sp}. The free energy values for surface interactions at different pH amounts are shown in Table 2. It can be seen that if the free energy amount was more negative, the interaction between particles surface and dispersant will be sufficient and the double layer electrical repulsion will be higher. The surface charge variations in the presence of dispersant with chemical adsorption mechanism can be quantitatively determined based on free specific energy of interaction (ΔG°_{sp}) and a relation between dispersion behavior and ΔG°_{sp} can be found.

In Table 2 it can be seen that ΔG°_{sp} at intermediate pHs 4–7 is more negative and it means that interaction between dispersant and particles surfaces is higher at these pH ranges, and at pHs of 2.5–4 dispersant effects decreased. So it could be concluded that APC dispersant increases sol stability based on interaction mechanism between dispersant and particles.

3.4. Study of particles size in sol

Fig. 4 shows the particles size variations at the beginning of the test and before the gelation point. As it can be observed, at low pH, the particles size is smaller at the beginning and after holding time because of very low concentration of OH$^-$ ions. In this condition, according to reaction (4), solubility rate is low. But at higher pH amounts, the OH$^-$ ions concentrations are increased which encourages the particle growth. In the sol system, due to existence of electric double layer around particles, they have electrostatic repulsive force. Thus, organic agents can be used for thickening adsorbing layers and for increasing the electrosteric stability in order to prevent from connection of very small particles. Electrosteric stability is a combination of electrostatic and steric repulsion and occurs due to adsorbing charged polymers on the surface. Probably, at long durations in sol processing, electrical charge decreasing and double layer thinning result in attraction between particles and agglomerates formation; Thus, the particle size increases. Electrosteric force by placing charged polymers on particles surface leads to increasing zeta potential and electrical repulsion. So as it is observed in Fig. 4, addition of dispersant APC into the sol increases the particles stability after holding time in comparison with sols without APC addition and this stability is more significant at intermediate pH 4–7 amounts. Fig. 5 illustrates the particles distribution at pH about 2.5 after and before sol aging. As it is seen, the particles have a narrow distribution and there is no particles dispersion inside the solution. Also, the particle size variations after aging are constant.

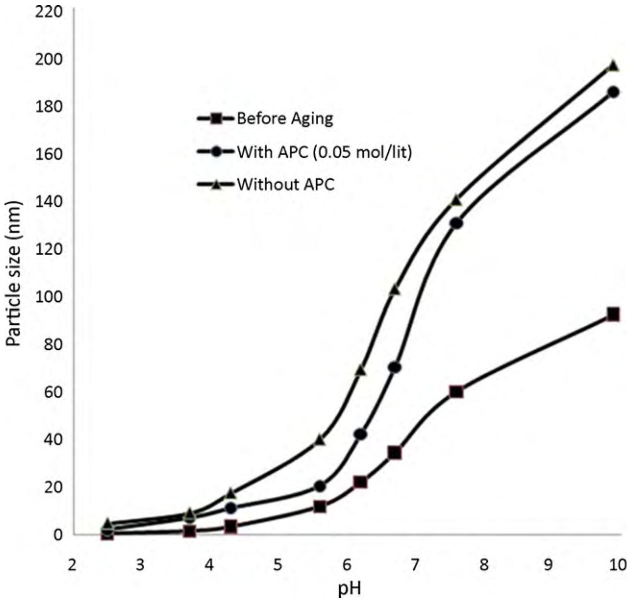

Fig. 4. Effect of pH on particle size.

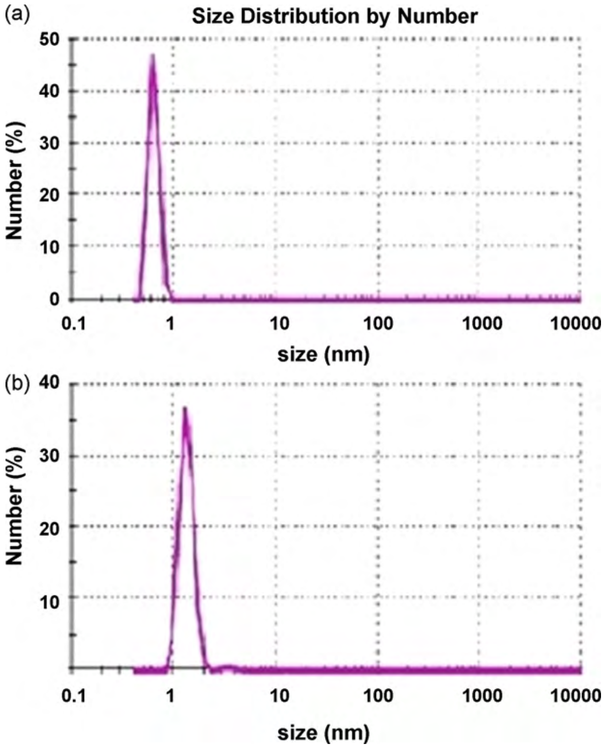

Fig. 5. Particle size distribution at pH 2.5 (a) before aging (b) and after gelation time.

3.5. Powder properties

The FTIR spectrum of the gel powder is shown in Fig. 6. As it is seen, siloxane bonds (Si–O-Si) which are formed by complete hydrolysis and condensation reactions of silicon alkoxides are observed at 498, 800 and 1090 cm^{-1}. A broad band at 3200 cm^{-1} corresponds to molecular water hydrogen-bonded to each other and to (Si-OH) groups. The bands observed around 2920 cm^{-1}, 1200–1456 cm^{-1} and 1393 cm^{-1}, respectively, are related to (C–H) bonds of methylene, (C–C) and (C–O) bonds, and (C=C) double bonds as well as aromatic loops which all are corresponded to phenolic resin bonds. It is noteworthy that there is a peak related to (Si–O–C) bonds at 754 cm^{-1} which is formed from phenolic resin carbon atoms connections with hydrolyzed and condensed TEOS (Si–O) bonds at molecular levels.

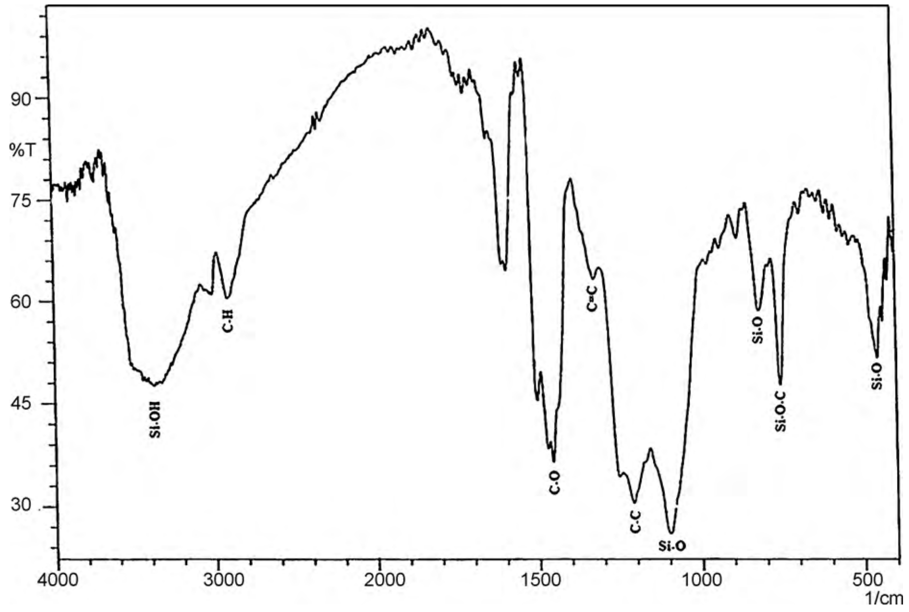

Fig. 6. FTIR spectrum of gel powder.

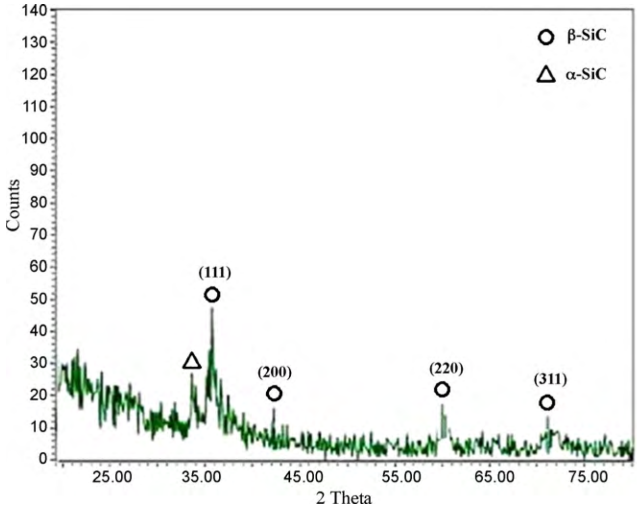

Fig. 7. X-ray diffraction pattern of synthesized SiC nanopowder at 1500 °C.

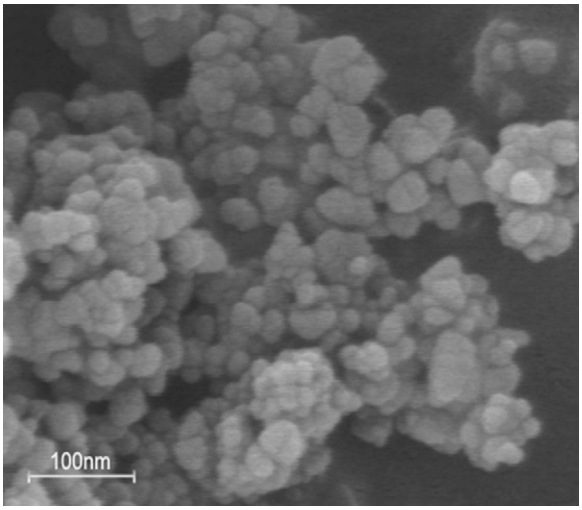

Fig. 8. SEM micrograph (FE-SEM) of synthesized SiC powder heat treated at 1500 °C.

Fig. 7 shows the X-ray diffraction pattern of synthesized powder with pH 2.5, APC 0.05 mol/l and heat treated at 1500 °C for 1 h. It can be seen that main peaks of synthesized powder at diffraction angles of (2θ) 35.6°, 41.3°, 60.1° and 72.1° are corresponded to (1 1 1), (2 0 0), (2 2 0) and (3 1 1) planes which are ascribed to cubic β-SiC phase. It should be noted that close to (1 1 1) planes peak between $2\theta = 33°$ and $2\theta = 35°$ there is a shoulder which is related to SiC hexagonal polytypes which are usually appeared as α-SiC (2H, 4H, 6H, etc.). Finally, no peak can be related to crystoballite and silica phases at XRD detection capability. The phase evaluation compares well with investigation carried out by Vix-Guterl et al. [22].

Fig. 8 exhibits the FE-SEM microstructure of synthesized powder. As can be seen in this figure, the produced powder is monosized and homogeneously distributed with semi-spherical morphology. The size of formed agglomerates is estimated to be less than 100 nm.

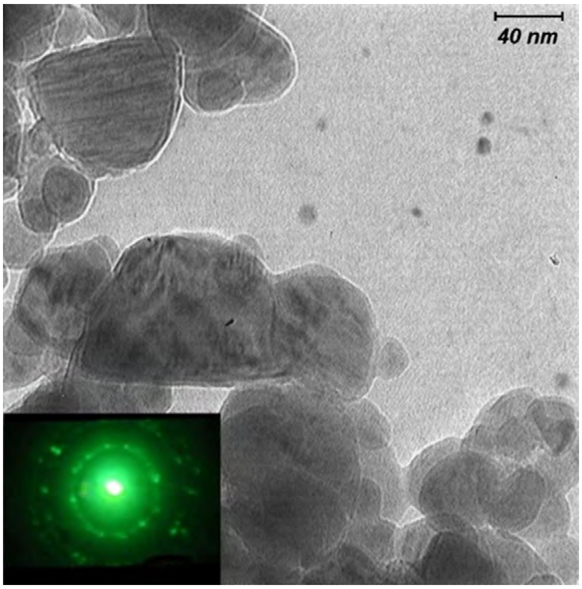

Fig. 9. TEM image and electron diffraction pattern of SiC powder heat treated at 1500 °C.

Fig. 9 shows transmission electron micrograph (TEM) of the synthesized powder with above characteristics. As it is illustrated, the mean size of the particles is between 30 and 50 nm. As the diffraction pattern of particles shows, these particles are polycrystalline at nanometric levels.

The particles were observed to grow as semi-spherical shape. This, we believe, is due to controlled processing parameters such as time and temperature which are maintained under equilibrium conditions. In fact we noticed, for example, the morphology of β-SiC particles changes to whisker type at long soaking time. Also at higher temperatures when CO or SiO gases evolve, the particles were found to grow in rod shape habit.

4. Conclusion

The effects of significant parameters on stability of suspension containing nanosize particles have been studied. The results showed that the surface charge on nanosize particles in the presence of APC dispersants is more negative at pH above 2.5 and the suspension tends to acidic conditions. Rheological measurements showed that the viscosity of sol increased at intermediate pH and decreased at extremely high and extremely low ones. This behavior was related to stability of sol in different conditions. The particles size could be controlled below 10 nm in the presence of APC dispersant at pHs lower than 4. The results of XRD analysis showed the β–SiC as a dominant phase with different crystalline planes. The microstructures resulted from SEM analysis indicated that the agglomerates size is less than 100 nm. Also the TEM results showed a size in the range of 30–50 nm for polycrystalline powders with semi-spherical morphology.

References

[1] M. Pierre, Surface Science Reports 48 (2002) 1–51.
[2] Q.G. Fu, H.J. Li, X.H. Shi, K.Z. Li, G.D. Sun, Scripta Materialia 52 (2005) 923–927.
[3] B.G. Ravi, O.A. Omotoye, T.S. Srivatsan, M. Petrorali, T.S. Sudarshan, Journal of Alloys and Compounds 299 (2000) 292–296.
[4] Y.-J. Lin, C.-M. Chuang, Ceramics International 33 (2007) 779–784.
[5] D. Kurtenbach, B.S. Mitchell, H. Zhang, M. Ade, E. Muller, Thermochimica Acta 337 (1999) 155–161.
[6] R. Koc, G. Glatzmaier, J. Sibold, Journal of Material Science 36 (2001) 995–999.
[7] R. Sharma, D.V. Sridhara Rao, V.D. Vankar, Materials Letters 62 (2008) 3174–3177.
[8] K.-i. Kurumada, H. Nakabayashi, T. Murataki, M. Tanigaki, Colloids and Surfaces A: Physicochemical and Engineering Aspects 139 (1998) 163–170.
[9] I. Seog, C.H. Kim, Journal of Material Science 28 (1993) 3277–3282.
[10] N. Sanz, A. Boudet, A. Ibanez, Journal of Nanoparticle Research 4 (2002) 99–105.
[11] G.H. Bogush, C.F. Zukoski, Journal of Colloid and Interface Science 142 (1991) 1–18.
[12] B.P. Singh, J. Jena, L. Besra, S. Bhattacharjee, Journal of Nanoparticle Research 9 (2007) 797–806.
[13] E. Vinogradova, M. Estrada, A. Moreno, Journal of Colloid and Interface Science 298 (2006) 209–212.
[14] J. Boucle, N. Herlin-Boime, A. Kassiba, Journal of Nanoparticle Research 7 (2005) 275–285.
[15] A. Ponton, S. Warlus, P. Griesmar, Journal of Colloid and Interface Science 249 (2002) 209–216.
[16] Z. Adamczyk, B. Jachimska, M. Kolasińska, Journal of Colloid and Interface Science 273 (2004) 668–674.
[17] F.J. Arriagada, K. Osseo-Asare, H.E. Bergna, Colloidal Silica-Fundamentals and applications, In: Horacio E. Bergna, William O. Roberts (eds.), Tailor and Francis, 2006, pp. 81–89.
[18] A.S. Zackrisson, A. Martinelli, A. Matic, J. Bergenholtz, Journal of Colloid and Interface Science 301 (2006) 137–144.
[19] H.-P. Martin, R. Ecke, E. Miiller, Journal of the European Ceramic Society 18 (1998) 1737–1742.
[20] H. Tamon, T. Kitamura, M. Okazaki, Journal of Colloid and Interface Science 197 (1998) 353–359.
[21] A. Einstein, Annalen der Physik 17 (1905) 549–560.
[22] C. Vix-Guterl, I. Alix, P. Ehrburger, Acta Materialia 52 (2004) 1639–1651.